Thermal Modeling of a Permanent Magnet Machine Built Using Litz Wire

Shafigh Nategh, Sigurd Øvrebø, Sara Mahdavi, *Member, IEEE*, Oskar Wallmark, *Member, IEEE*

***Abstract*—This paper considers thermal modeling of a 2 MW permanent magnet machine designed and manufactured for marine applications. The main focus is placed on the winding made of the Litz wire, and a practical approach to model heat transfer is presented. The proposed thermal modeling method, named segment-layer, is compared to traditional thermal models used mainly for standard winding configurations. In order to evaluate the accuracy of the developed thermal model, both simulation and experimental results are presented. In the simulation study, the proposed and traditional modeling methods are compared to a detailed finite element model of the Litz wire. Temperature measurements are carried out on the 2 MW machine prototype and a good agreement between the measurements and corresponding thermal model results is achieved. The suggested method is user-friendly and enables both analytical and numerical modeling of the Litz wire. Also, the parameters that play an important role in the winding heat transfer, e.g. impregnation goodness, can be easily implemented in the model developed in this paper.**

***Index Terms*—Finite element (FE), impregnation goodness, Litz wire, lumped parameter thermal model, permanent magnet (PM) machines.**

I. Introduction

In electric machines designed for high-performance applications, e.g. marine and aerospace industries, a high torque and power density is essential. A high torque density in permanent magnet machines can be achieved by applying a higher current to the stator winding and/or using high-grade magnets in the rotor structure. A higher current density in the stator slots results in a considerable amount of copper losses in the winding and, consequently, a high temperature in the stator slots and the end windings [1].

Both windings and rotor mounted permanent magnets are machine critical parts from a thermal point of view. The magnet remanent flux density is dependent on the temperature and an unexpected increase in the magnet temperature reduces the remanent flux density which directly influences the torque. As a consequence, to fulfill the required torque, a higher current should be applied to the winding that, in turn, increases the winding temperature and reduces the machine efficiency. Additionally, very high temperatures can result in permanent partial/total demagnetization of the magnets [2]. A high temperature in the winding increases copper losses and reduces the insulation lifetime.

An accurate estimation of the machine temperature distribution is necessary for successful electromagnetic and cooling system design. Otherwise, the design process may end up in a very compact solution suffering from a high temperature in the machine's critical parts which significantly affects the machine performance. Another alternative is to have an oversized design which is not acceptable.

In the last decades, many attempts have been made with the aim of developing functioning thermal models for electric machinery. Lumped parameter (LP) and numerical methods are the major thermal modeling approaches used in electric machinery applications. The LP model is an analytical method where distributed fields are considered as a limited number of single scalars. As a result, a quick thermal analysis can be carried out providing fairly accurate results provided that the LP network parameters are calculated correctly [3]–[5]. Finite element (FE) and computational fluid dynamics (CFD) are the numerical methods employed for thermal modeling of electrical machines [6], [7]. In a FE model, the conductive heat transfer in the solid parts can be modeled accurately. However, radiation and convection must be modeled as boundary conditions estimated using analytical models [7], [8]. CFD analysis can be used to precisely model fluid flow and also convective heat transfers. It should be noted that implementing and running FE and CFD models considering the complex structure of the electric machines can be very time-consuming [9], [10].

As mentioned above, the winding is one of the most critical parts of the machine. The thermal models developed for this part of the machine are mainly based on homogenization and multi-layer structure. The homogenization method is presented by Idoughi et al. in [11] where the influence of key parameters, e.g. the slot fill factor is studied in detail. The multi-layer model for the winding proposed in [12] by Staton et al. enables estimation of the winding hot spot temperature.

A. Contributions and Outline of Paper

New types of the Litz wire have recently been used as a solution for winding designs in compact machines operating at high frequencies where proximity and skin effects in traditional winding configurations can cause serious problems [13], [14]. However, the Litz wire structure can make heat dissipation from the turns located close to the slot center difficult. Consequently, an accurate thermal model of the Litz wire arrangement in the design stage should be implemented to ensure that the winding temperature will not affect the machine life-time and electromagnetic performance.

Shafigh Nategh and Sigurd Øvrebø are with SmartMotor AS, Rolls-Royce Group, Trondheim, Norway (e-mail: {shafigh, sigurdo}@smartmotor.no).

Sara Mahdavi is with Department of Electrical Machines, RWTH Aachen University, Germany.

Oskar Wallmark is with Department of Electrical Energy Conversion, KTH Royal Institute of Technology, Stockholm, Sweden.

978-1-4799-7400-9/15/$31.00 ©2015 IEEE

Authorized licensed use limited to: Universitaetsbibliothek der RWTH Aachen. Downloaded on August 19,2020 at 10:07:33 UTC from IEEE Xplore. Restrictions apply.

In this paper, thermal modeling of a water-cooled permanent magnet machine built using Litz wire is presented. First, available thermal models for traditional winding configurations are presented. Then, an alternative thermal modeling method is proposed for the Litz wire arrangement used in the studied machine. In order to evaluate the accuracy of the modeling approaches presented in this paper, a finite element (FE) thermal model of the Litz wire including all the details is implemented.

Also, a 2 MW prototype equipped with a number of temperature sensors is built and tested. A good correspondence between the thermal model results and measurements is observed.

II. Thermal Modeling of Standard Winding

As discussed in the introduction, homogenization and layered structures are the main thermal modeling approaches proposed for traditional windings. As presented in [11], the model proposed based on homogenization underestimates the winding hot spot temperature, especially at low slot fill factors. Also, it does not include the end winding part.

Multi-layer modeling is based on dividing the slot into a number of elliptical/rectangular impregnation, copper and liner layers as shown in Fig. 1 [15]. Since the thermal conductivity of copper is considerably higher than the thermal conductivity of the impregnation material filling the stator slots, the temperature variation in the copper layers can be neglected and heat transfer in the impregnation/liner layers is only considered.

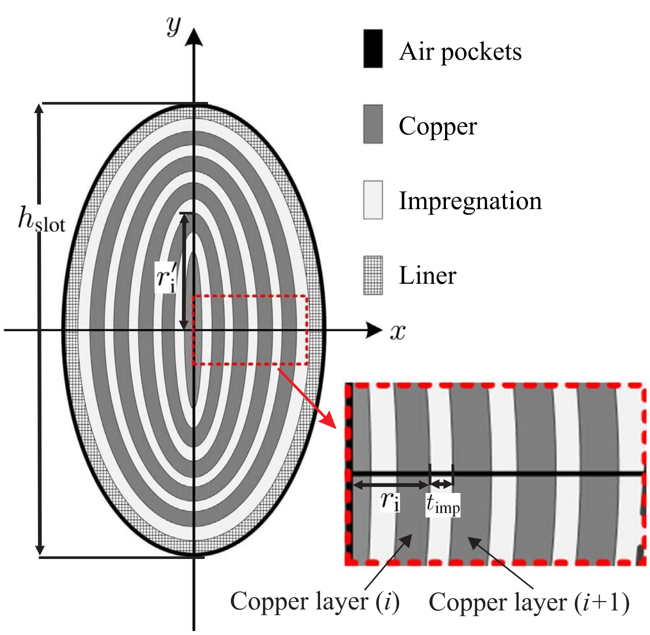

Fig. 1: The adopted elliptical model of the winding active part [15].

III. Thermal Modeling of Litz Wire

In machines operating at high frequencies, the influence of skin and proximity effects on the copper losses produced in the winding can be significant. One solution is to use Litz wire where each turn is divided into a high number of thin conductors. However, the many turn insulations used in the winding structure make the heat transfer from the slot center to the slot wall difficult which can lead to a high temperature in the winding [16]. Additionally, the Litz wire structure including the turn insulations and a high number of thin conductors hinders an effective penetration of impregnation material into the stator slots and the end winding which can result in a low impregnation goodness[1]. A lower impregnation goodness means that the amount of air pockets with a low thermal conductivity introduced in the impregnation body during the vacuum pressure impregnation (VPI) process is high.

Due to the abovementioned reasons, an accurate thermal model of the winding including the Litz wire key factors and details, e.g., impregnation goodness and turn insulations, should be developed. In the sections below, available winding models are applied to the Litz Wire. Also, an alternative model named *segment-layer* is presented.

A. Detailed Litz Wire Model

In order to investigate the accuracy of the modeling methods presented in the following sections, a detailed thermal model of the Litz wire is first developed. Such a model is demonstrated in Fig. 2. As shown, the model consists of many thin copper strands with a diameter of 0.03–0.5 mm. The copper strands are ideally surrounded by the impregnation material although air pockets are expected, especially in the cases that the standard VPI is replaced by vacuum and dipping processes. Also, some layers of turn insulation are considered and the entire coil is covered by the slot liner or alternatively some layers of the main wall insulation. Finally, a contact surface between the main wall insulation and stator steel laminations is included.

This model is difficult to implement analytically, e.g. as a LP model. Additionally, putting this winding model into a FE or CFD model of the complete machine results in an extremely high number of model elements and, in turn, a very long computation time.

B. Litz Wire Model Based on Homogenization

In this thermal modeling method, the copper conductors, impregnation material and turn insulations are considered as a homogenous body with a specified equivalent thermal conductivity. The following equations are suggested to estimate the equivalent thermal conductivity of a two-component body. For simplification, since the thermal conductivity of the impregnation material is close to the thermal conductivity of the turn insulations, slot liner and slot wedge, they can be considered as a single component. The second component is then copper. Thereby, the equivalent thermal conductivity can be calculated using the slot fill-factor as follows.

$$\lambda_{\text{eq}} = \lambda_{\text{ins}} \frac{\lambda_{\text{cu}}(1+FF) + \lambda_{\text{ins}}(1-FF)}{\lambda_{\text{cu}}(1-FF) + \lambda_{\text{ins}}(1+FF)} \tag{1}$$

[1]The impregnation goodness represents the volume of impregnation material over the total volume of the impregnation body including the air pockets and impregnation material.

Authorized licensed use limited to: Universitaetsbibliothek der RWTH Aachen. Downloaded on August 19,2020 at 10:07:33 UTC from IEEE Xplore. Restrictions apply.

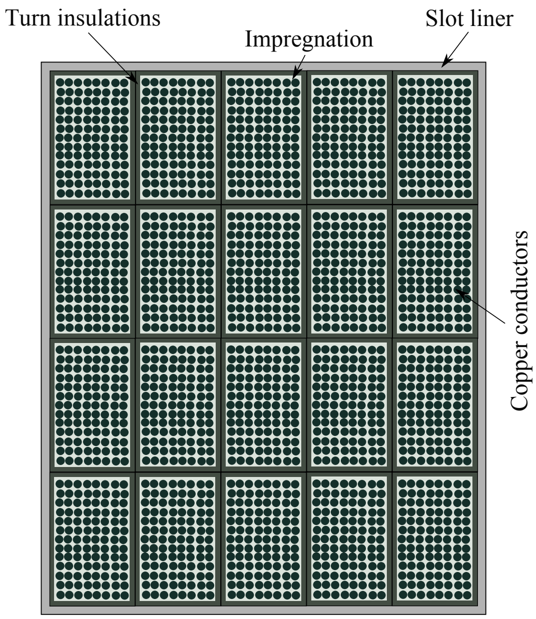

Fig. 2: Litz wire configuration with 20 turns in the form of 4×5.

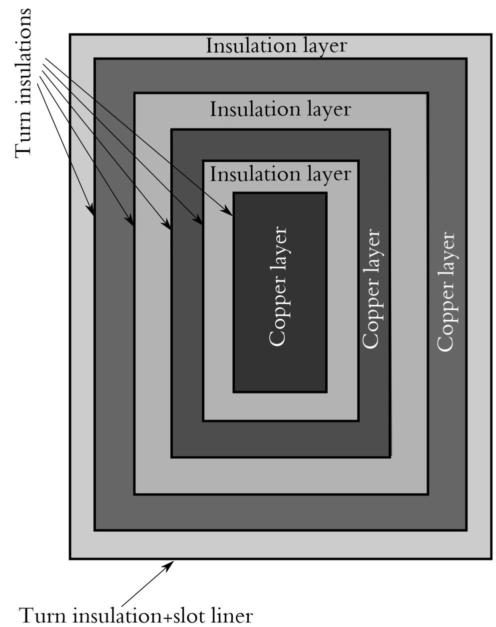

Fig. 3: multi-layer model of the Litz wire.

Here, λ_{ins} is the thermal conductivity of the material used in the stator slot except from the copper strands. FF is the stator fill factor and λ_{cu} is the copper thermal conductivity.

In order to calculate the equivalent thermal conductivity λ_{eq} with a higher accuracy, the following equation can be employed where an additional factor k is included. This equation has a higher accuracy particularly at low slot fill-factors.

$$\lambda_{\text{eq}} = \lambda_{\text{ins}} \frac{(\Delta_{\text{FF}}\lambda_{\text{ins}} + FF\lambda_{\text{cu}} + \lambda_{\text{cu}})(\lambda_{\text{ins}} + \lambda_{\text{cu}}) - k\Delta_{\text{FF}}(\Delta_{\lambda})^2}{(FF\lambda_{\text{ins}} + \Delta_{\text{FF}}\lambda_{\text{cu}})(\lambda_{\text{ins}} + \lambda_{\text{cu}}) - k\Delta_{\text{FF}}(\Delta_{\lambda})^2} \quad (2)$$

Here, Δ_{FF} and Δ_{λ} are equal to $(1 - FF)$ and $(\lambda_{\text{cu}} - \lambda_{\text{ins}})$, respectively. The factor k can be found from the below table [11].

TABLE I: k as a function of slot fill factor.

Fill factor	0.3	0.4	0.5	0.6	0.65
k	0.092	0.121	0.165	0.251	0.375

C. Multi-Layer Litz Wire Model

In this approach [15], the Litz wire is modeled similar to the standard winding model presented in Section II. The main difference is the turn insulations that are applied to the layer boundaries. The developed model configuration can be found in Fig. 3.

D. Segment-layer Litz Wire Model

In the segment-layer model presented in Fig. 4, the Litz wire turn boundaries are kept unchanged and a single layer model is applied to the copper and impregnation. The proposed model avoids simulating a very high number of copper conductors

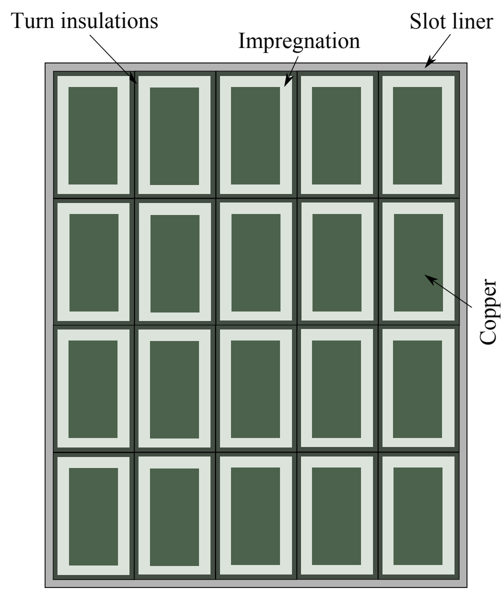

Fig. 4: Segment-layer model of the Litz wire.

while the Litz wire main structure is still identical to the real Litz wire configuration. Also, the model can be easily implemented in a FE thermal tool where the winding layers are implemented as *thin conductive layers*. Consequently, a convenient but accurate model of the Litz wire arrangement is realized where the complex structure of the Litz is simplified to a number of rectangular blocks. Since the rectangular blocks presented in Fig. 4 are made of copper with a high thermal conductivity, the temperature variation in each block is very small and a very coarse mesh is needed. As a result, the developed model when implemented in a FE tool uses a very low number of elements and the required computation time can be kept short.

1) FE/CFD Model Implementation: As shown in Fig. 4, the proposed segment-layer model simplifies the winding structure

Authorized licensed use limited to: Universitaetsbibliothek der RWTH Aachen. Downloaded on August 19,2020 at 10:07:33 UTC from IEEE Xplore. Restrictions apply.

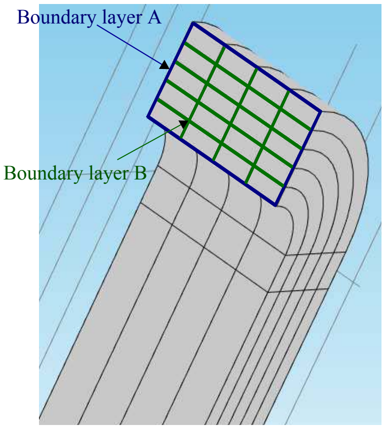

Fig. 5: Developed segment-layer model of the Litz wire in the finite element tool.

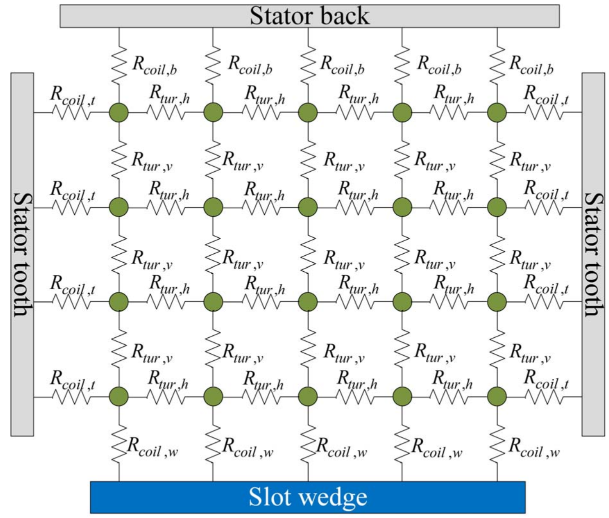

Fig. 6: Developed LP model of the segment-layer configuration.

by removing the small copper strands. However, still the very thin turn insulations, slot liner and contact surfaces require very small element sizes in the FE model that, in turn, increase the model size and the needed computation time. In order to overcome this issue, one can suggest using *thin conductive layers* available in many thermal FE tools. Under this condition, a very coarse mesh is utilized to model the heat transfer in the copper layers with high thermal conductivity where a small temperature variation is expected. Also, the heat transfer in the thin turn insulations and slot liners is modeled using boundary conditions. Consequently, the model size is very small enabling an accurate estimation of the hot spot temperature in a short computation time. Such a model can be found in Fig. 5 and the key parameters used are drawn as follows.

The boundary layer A between the copper and stator laminations includes: 1- the contact surface between the lamination and winding with the thermal conductivity of $0.03\ W/m.K$ and an equivalent length of 0.01-0.1 mm based on the winding process quality, 2- slot liner with the thickness of L_{liner} and thermal conductivity of $0.3\ W/m.K$, 3- one layer turn insulation with the thickness of L_{turn} and a thermal conductivity of 0.3 $W/m.K$, and 4- impregnation layer L_{imp} obtained based on the slot fill factor as follows.

$$FF_{\text{slot}} = \frac{N_{\text{turn}} W_{\text{cu}} H_{\text{cu}}}{W_{\text{slot}} H_{\text{slot}}} \quad (3)$$

where W_{slot} and H_{slot} are the slot width and height, respectively, and N_{turn} is the total number of turns in a slot. Also, W_{cu} and H_{cu} are defined as follows.

$$W_{\text{cu}} = (W_{\text{slot}} - 2L_{\text{liner}})/N_{\text{W}} - 2L_{\text{imp}} - 2L_{\text{turn}} \quad (4)$$

$$H_{\text{cu}} = (H_{\text{slot}} - L_{\text{wedge}} - 2L_{\text{liner}})/N_{\text{H}} - 2L_{\text{imp}} - 2L_{\text{turn}} \quad (5)$$

where N_{W} and N_{H} are the number of turns along the slot width and height, respectively. L_{wedge} is the slot wedge thickness.

The boundary layer B includes two layers of turn insulation with the thickness L_{turn} and two impregnation layers with the thickness L_{imp}. Also, based on the coil assembly and impregnation quality, another contact surface between the turns may be considered.

In the case that the 'thin conductive layer' boundary is not available in the used numerical tool package, the FE/CFD model can be combined with analytical models where boundaries A and B are modeled using thermal resistances between the copper surfaces.

2) LP Model Implementation: The model can also be simply implemented into an analytical thermal model. In this case, the copper blocks are represented by the nodes and the thermal resistances are used with the aim of modeling the impregnation material, turn insulations, slot liners and contact surfaces, e.g. the contact surface between the stator slot and steel laminations. Such a model is presented in Fig. 6. Here, $R_{\text{tur, h}}$ and $R_{\text{tur, v}}$ represent the vertical and horizontal thermal resistances between the turns including the turn insulations, impregnation layers and contact surfaces between the turns. The thermal resistances between the outer turns and stator laminations are represented by $R_{\text{coil, b}}$ and $R_{\text{coil, t}}$. These resistances contain the turn insulation, impregnation layer, slot liner (or main wall insulation) and contact surface between the coil and steel laminations. $R_{\text{coil, w}}$ represents heat transfer between the turns located at the bottom of the slots and the slot wedge.

The same model can be applied to both active part of the winding and the end winding. The only difference is in the outer thermal resistances ($R_{\text{coil, b}}$, $R_{\text{coil, t}}$, $R_{\text{coil, w}}$), where the slot liner and the contact surfaces are replaced by the convective heat transfers from the end winding surface to the fluid covering the end winding [4], [7].

E. Comparison Between the Proposed Models

In order to evaluate the accuracy of the developed models, a comparison between the estimated hot-spot temperatures using the suggested models and the detailed model in Section III-A is presented. The evaluation is carried out for the Litz wires with two different strand shapes and slot fill factors. In the results presented in Fig 7, the round strands are considered and the resulting slot fill factor is approximately 0.47. In Fig. 8,

Authorized licensed use limited to: Universitaetsbibliothek der RWTH Aachen. Downloaded on August 19,2020 at 10:07:33 UTC from IEEE Xplore. Restrictions apply.

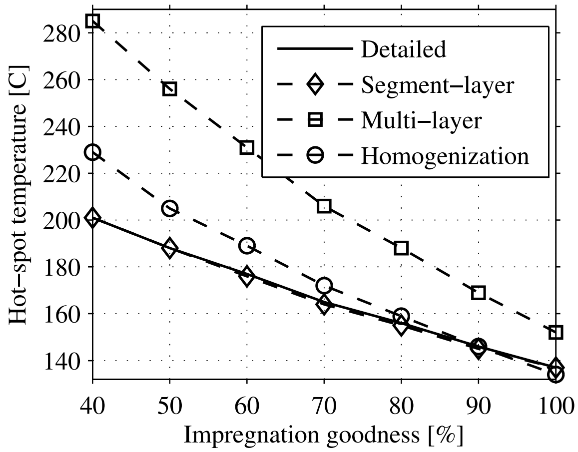

Fig. 7: A comparison between the estimated hot spot temperatures using the models developed for Litz wire. the Litz wire is made of round strands and the resulted slot fill factor is 0.47.

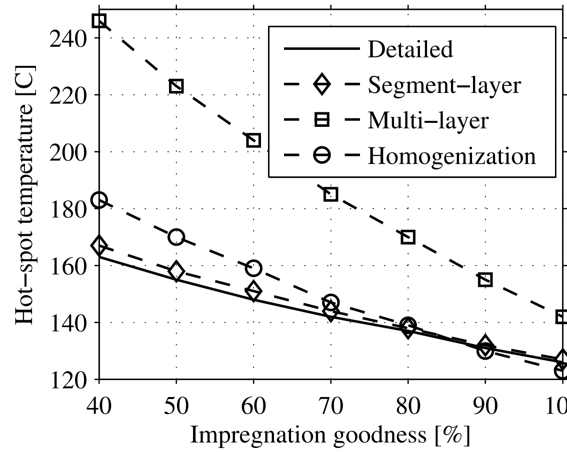

Fig. 8: A comparison between the estimated hot spot temperatures using the models developed for Litz wire. the Litz wire is made of rectangular strands and the resulted slot fill factor is 0.58.

different models for a Litz wire with rectangular strands and a slot fill factor of approximately 0.58 are evaluated.

As shown in Fig. 7, the multi-layer model developed for the round strand Litz wire estimates the winding hot spot temperature with the highest error. The calculated error is 11% at an impregnation goodness of 100% and 42% at an impregnation goodness of 40%. Despite the standard winding, the model proposed based on homogenization has a higher accuracy than the multi-layer model. This model has a fairly good accuracy especially at higher impregnation goodness values. However, at an impregnation goodness of 40%, the error has increased to 14%. This error will increase even more at lower impregnation goodness values. As can be seen, the proposed segment-layer model perfectly follows the detailed model in the entire range of impregnation goodness levels.

For a Litz wire made of rectangular strands and with a fill factor of 0.58 (see Fig. 8), the multi-layer model estimates the hot spot temperature with an error of 52% which is 10% higher than the Litz wire model discussed above. The model developed based on homogenization has a relatively higher accuracy in this case compared to Litz wire made of round wire. The proposed segment-layer model still follows the detailed models with only minor deviations.

IV. Comparison with Experimental Results

A 2 MW permanent magnet machine made using Litz wire and equipped with a number of thermocouple and PT100 sensors is considered as the case study. The stator including the winding is water cooled while the rotor is cooled by two fans mounted on the non-drive end-cap. The coils are impregnated using a VPI process and sensors are placed in the winding at different locations, mainly in the end winding where the machine hot spot temperature is expected. The data acquisition system used is Agilent[2] 34970A.

[2]Agilent is a registered trademark of the Agilent Technologies, Inc., Santa Clara CA 95051, United States.

Fig. 9: The 2 MW permanent magnet machine studied.

A. *Loss Estimations: Complete 3DFEM Model*

Losses as the input of the thermal model play an important role in the model verification. The electromagnetic FE analysis tool, JMAG[3], is used with the aim of loss calculations in the studied machine. Developed 3D model provides an accurate estimation of the produced eddy current losses in the magnet segments, housing and rotor support ring. Also, the hysteresis losses produced in the rotor and stator steel laminations are calculated using the full hysteresis curve of the material used and the flux density variations calculated by the 2D FE modeling of the machine. The eddy current losses produced in the steel laminations are calculated based on the thickness and conductivity of the steel lamination together with the calculated flux density.

B. *Thermal Model of the Complete Machine*

The developed thermal model of the Litz wire detailed in Section III-D is used in the thermal model of the complete

[3]JMAG is a registered trademark of the JSOL Corporation, Tokyo, Japan.

Authorized licensed use limited to: Universitaetsbibliothek der RWTH Aachen. Downloaded on August 19,2020 at 10:07:33 UTC from IEEE Xplore. Restrictions apply.

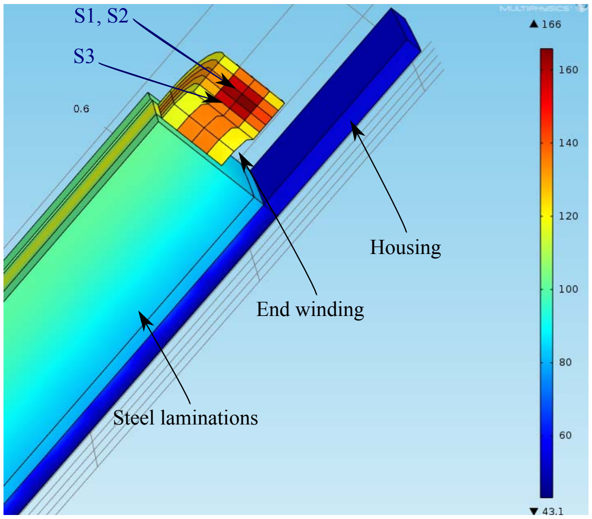

Fig. 10: Thermal FE modeling results: machine stationary parts.

machine. The model includes the winding, stator laminations, housing and the rotor. The cooling system including the housing water jacket and the rotor air cooling is implemented using convective heat transfer boundary conditions.

C. Experimental Evaluation

A comparison between the measurements and the estimated temperatures of the winding using the segment-layer model detailed in Section III-D is presented in Fig. 10 and Table II. As can be seen, the winding includes four and five layers along the height and width of the slot, respectively. End winding sensors are placed between the turns, where sensor 1 and 2 (S1, S2) are located close to the winding center. Sensor locations are also presented in the Fig. 10.

TABLE II: Comparison between thermal model results and corresponding measurements.

Sensor location	Model	Meas.
End winding sensor 1 (Drive end)	158.0	155.0
End winding sensor 2 (Non-drive end)	157.3	155.0
End winding sensor 3	137.0	132.0
Outside the end winding	126.0	122.0
Inside the slot (close to the wedge)	125.0	123.0

V. Conclusion

In this paper, a practical and functioning thermal model is proposed for the Litz wire. It is found that previously reported models are not able to accurately estimate the Litz wire hot-spot temperature with a high accuracy, particularly when the quality of the impregnation process is not ideal. Also, an alternative thermal model, named *segment-layer*, is developed that enables estimation of the Litz wire temperature distribution with a high accuracy. It should be noted that the developed model is functioning and can be applied to both numerical and analytical thermal models as elaborated in the paper. The model is tested at a wide range of the impregnation goodness values (40% to 100%), and for two different Litz wire configurations with round and rectangular copper strands. It is found that the model has a higher accuracy in the Litz wires with round strands and slightly overestimates the hot-spot temperature in the Litz wire made of the rectangular copper strands. Finally, experimental tests on a 2 MW PM machine prototype, that its winding is made of the Litz wire, are carried out. A good agreement between the predicted and measured temperatures is obtained.

References

[1] C. Gerada, K. Bradley, C. Whitley, and G. Towers, "High torque density PM machines for high performance operation," in *33rd Annual Conference of the IEEE Industrial Electronics Society*, Nov. 2007, pp. 210 –215.

[2] P. Zhou, D. Lin, Y. Xiao, N. Lambert, and M. A. Rahman, "Temperature-dependent demagnetization model of permanent magnets for finite element analysis," *Magnetics, IEEE Transactions on*, vol. 48, no. 2, pp. 1031–1034, Feb 2012.

[3] A. Boglietti, A. Cavagnino, and D. Staton, "TEFC induction motors thermal models: a parameter sensitivity analysis," *IEEE Transactions on Industry Applications*, vol. 41, no. 3, pp. 756–763, 2005.

[4] A. Boglietti and A. Cavagnino, "Analysis of the endwinding cooling effects in TEFC induction motors," *IEEE Transactions on Industry Applications*, Sept.-oct. 2007.

[5] A. Boglietti, A. Cavagnino, D. Staton, M. Popescu, C. Cossar, and M. McGilp, "End space heat transfer coefficient determination for different induction motor enclosure types," *IEEE Transactions on Industry Applications*, vol. 45, no. 3, pp. 929–937, May-june 2009.

[6] A. Boglietti, A. Cavagnino, D. Staton, M. Shanel, M. Mueller, and C. Mejuto, "Evolution and modern approaches for thermal analysis of electrical machines," *IEEE Transaction on Industrial Electronics*, vol. 56, no. 3, pp. 871–882, March 2009.

[7] D. A. Staton and A. Cavagnino, "Convection heat transfer and flow calculations suitable for electric machines thermal models," *IEEE Transactions on Industry Applications*, vol. 55, no. 10, pp. 3509–3516, Oct. 2008.

[8] J. Wang, F. Wang, and X. Kong, "Losses and thermal analysis of high speed pm machine," in *Power System Technology and IEEE Power India Conference, 2008. POWERCON 2008. Joint International Conference on*, Oct 2008, pp. 1–5.

[9] C. Kral, A. Haumer, M. Haigis, H. Lang, and H. Kapeller, "Comparison of a CFD analysis and a thermal equivalent circuit model of a TEFC induction machine with measurements," *IEEE Transactions on Energy Conversion*, vol. 24, no. 4, pp. 809–818, Dec. 2009.

[10] D. Howey, A. Holmes, and K. Pullen, "Measurement and CFD prediction of heat transfer in air-cooled disc-type electrical machines," *Industry Applications, IEEE Transactions on*, vol. 47, no. 4, pp. 1716–1723, July 2011.

[11] L. Idoughi, X. Mininger, F. Bouillault, L. Bernard, and E. Hoang, "Thermal model with winding homogenization and FIT discretization for stator slot," *IEEE Transactions on Magnetics*, vol. 47, no. 12, pp. 4822 –4826, Dec. 2011.

[12] D. Staton, A. Boglietti, and A. Cavagnino, "Solving the more difficult aspects of electric motor thermal analysis in small and medium size industrial induction motors," *IEEE Transactions on Energy Conversion*, vol. 20, no. 3, pp. 620–628, Sept. 2005.

[13] H. Hamalainen, J. Pyrhonen, J. Nerg, and J. Talvitie, "Ac resistance factor of litz-wire windings used in low-voltage high-power generators," *Industrial Electronics, IEEE Transactions on*, vol. 61, no. 2, pp. 693–700, Feb 2014.

[14] H. Rossmanith, M. Doebroenti, M. Albach, and D. Exner, "Measurement and characterization of high frequency losses in nonideal litz wires," *Power Electronics, IEEE Transactions on*, vol. 26, no. 11, pp. 3386–3394, Nov 2011.

[15] S. Nategh, O. Wallmark, M. Leksell, and S. Zhao, "Thermal analysis of a PMaSRM using partial FEA and lumped parameter modeling," *IEEE Transactions on Energy Conversion*, vol. 27, no. 2, pp. 477–488, June 2012.

[16] S. Nategh, A. Krings, O. Wallmark, and M. Leksell, "Evaluation of impregnation materials for thermal management of liquid-cooled electric machines," *Industrial Electronics, IEEE Transactions on*, vol. 61, no. 11, pp. 5956–5965, Nov 2014.

Authorized licensed use limited to: Universitaetsbibliothek der RWTH Aachen. Downloaded on August 19,2020 at 10:07:33 UTC from IEEE Xplore. Restrictions apply.